



ISSN: 0067-2904

## Well Log Analysis and Interpretation for Khasib, Tanuma, and Sa'di formations for Halfaya Oil Field in Missan Governorate-Southern Iraq

Arjwan Hamid Fayadh\*, Mad'hat E. Nasser

Department of Geology, College of Science, University of Baghdad, Baghdad, Iraq.

### Abstract

The study intends to interpretation of well logs to determine the petrophysical parameters for Khasib, Tanuma, and Sa'di formations in Halfaya Oil Field. Where this field is located 30 kilometers south-east of the Amara city and it is considered as one of the important fields in Iraq because of the high production of oil, because Khasib, Tanuma, and Sa'di are f carbonates reservoirs formations and important after the Mishrif Formation because of the lack of thickness of the formations compared to the amount of oil production. The Matrix Identification (MID) and the M-N crossplot were used to determine the lithology and mineralogy of the formations; through the diargm it was found the three formations consisted mainly of calcite with some dolomite. Density – Neutron cross plot for lithology identification which shows that the formations are mainly consist of limestone with little shale.

**Keywords:** petrophysical parameters, reservoirs, crossplot.

### تحليل وتفسير الجس البئري لتكاوين خصيب، تنومه، وسعدي في حقل الحلفاية النفطي في محافظة ميسان \_ جنوب العراق

أرجوان حامد فياض\*، مدحت عليوي ناصر

قسم علم الارض، كلية العلوم، جامعة بغداد، بغداد، العراق.

### الخلاصة

تهدف الدراسة الى تفسير مجسات الابار وتحديد الخواص البتروفيزيائية لتكاوين خصيب، تنومه، وسعدي في حقل الحلفاية النفطي. حيث يقع هذا الحقل على بعد 30 كيلومتر جنوب شرق مدينة العمارة ويعتبر واحدا من الحقول المهمة في العراق بسبب الانتاج العالي من النفط وتعتبرتكاوين خصيب، تنومه، وسعدي تكاوين كاربونية منتجة ومهمه بعد تكوين مشرف الكاربوني بسبب قلة سمك التكاوين مقارنة مع كمية الانتاج النفطي. تم استخدام (MID and M-N cross plots) لتحديد الصخرية والمعدنية للتكاوين؛ من خلال المرسمات تم التوصل الى ان التكاوين الثلاثة تتكون بشكل رئيسي من الكالساييت calcite مع القليل من الدولومايت dolomite. بينما تم استخدام (Density – Neutron cross plot) لتحديد الصخرية وتبين ان التكاوين تتكون اساسا من الحجر الجيري limestone مع القليل من الطفل shale.

### Introduction

Khasib, Tanuma, and Sa'di formations are carbonate sequence were deposited during the Cretaceous period in the secondary sedimentary cycle (The Turonian-Lower Campanian). This carbonate sequence comprises many shale and marl units alternating with some porous and fractured

\*Email: hbeara1993@yahoo.com

carbonate unites in some oil [1]. The Halfaya oil field in the Mesopotamian basin trend in NW-SE. The Arabian Gulf Basin was mainly influenced by the Alps Tectonic Movement, and developed the platform deposition. The platform within Iraqi territory can be divided into two large tectonic zones from west to east, the stable continental shelf zone in the west and unstable continent shelf zone in the east. Halfaya Oil field in Iraq is located in the unstable continental shelf on the northern of Arabian Gulf Basin. Huge thick sedimentary strata covered the unstable continent shelf [2]. The Kometan Formation is the most widespread Turonian formation of northern and central Iraq, which should represent partly the age equivalents of the former three formations [3].

### Study Area

The Halfaya field is located in southern Iraq in Missan governorate, 30 kilometers southeast Amara city [Figure-1]. Area was the first surveyed in 1957 and then the national oil company has performed seismic survey which covered the region during the period 1973. Appearance results for Halfaya structural form is pear shape consists of two domes extending from the northwest to the south-east.

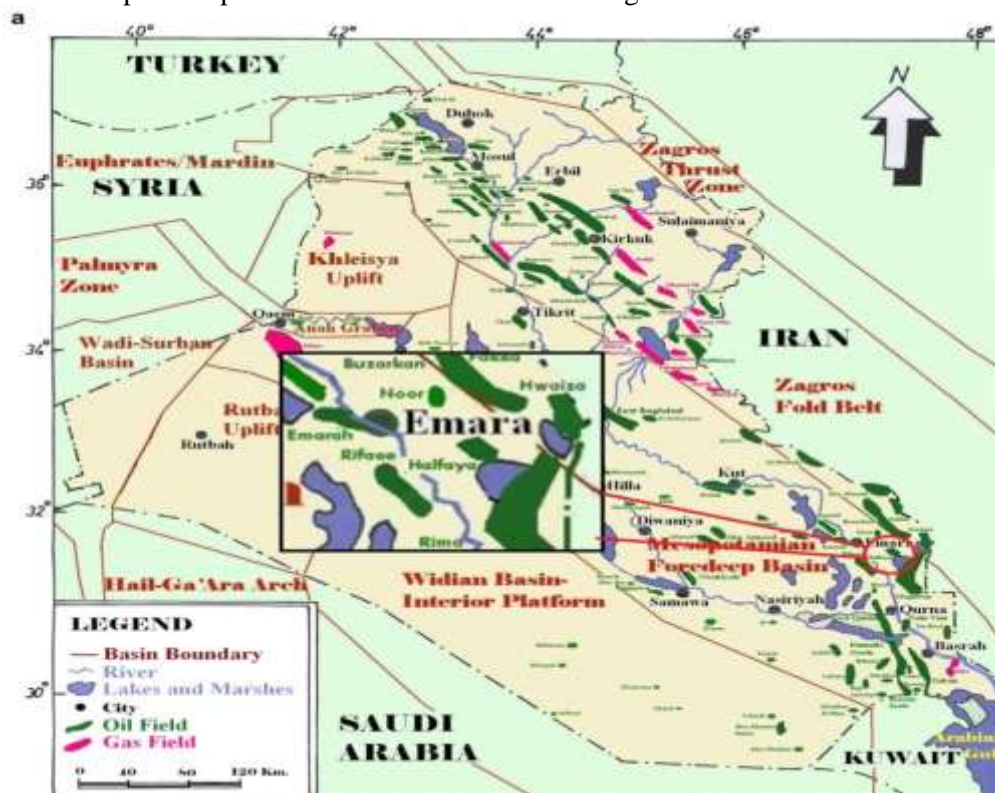


Figure 1-Location map of Halfaya oil field [4].

The main purpose of the present study is interpretation of well logs to determine the petrophysical parameters for Khasib, Tanuma, and Sa'di formations and evaluating the petrophysical properties of these formations using available core analysis.

### Methodology

The data were used from available records (LAS) such as potential spontaneous records (SP), gamma rays, density, sonic, neutrons, and resistivity. Loaded into the IP program and calculating the water saturation ratio and moveable hydrocarbons as well as the effective and secondary porosity, lithology and mineralogy for the three formations.

### Borehole Environment

During the drilling of the well the hydrostatic pressure of the mud column is usually greater than the pore pressure of the formations. This prevents the well from "blowing out". The resultant differential pressure between the mud column and formation forces mud filtrate into the permeable formation, and the solid particles of the mud are deposited on the borehole wall where they form a mudcake [Figure-2]. Mudcake usually has a very low permeability (of the order of  $10^{-2}$ - $10^{-4}$  md) and,

once developed, considerably reduces the rate of further mud filtrate invasion to very close to the borehole and most of the original formation water and some of the hydrocarbons may be flushed away by the filtrate. This zone is referred to as the flushed zone [5].

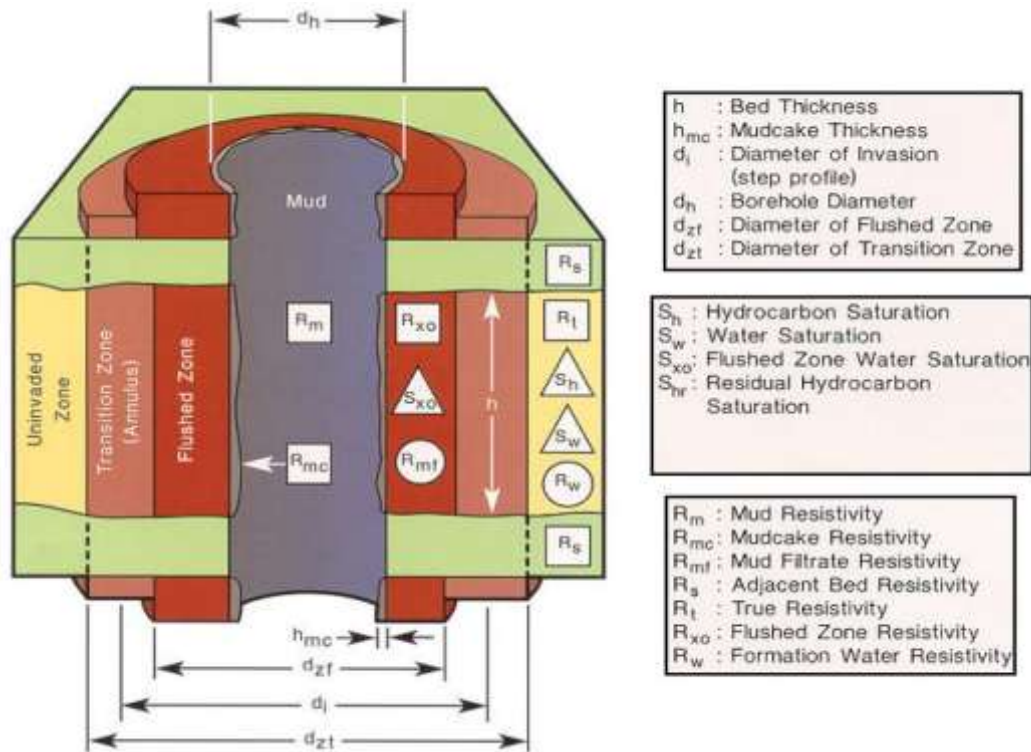


Figure 2- Illustrating the borehole environment [6].

### Resistivity log

Resistivity logs are electric logs, which are the oldest geophysical logging techniques, introduced by the Schlumberger brothers in oil and gas exploration [7]. The resistivity of a substance has ability to impede the flow of electric current through that substance [8]. The resistivity of a formation is the key parameter in determining hydrocarbon saturation. The resistivity of formation depends on resistivity of the formation water, amount of water present, and pore structure geometry [5].

### Spontaneous Potential Log (SP)

The SP curve records the electrical potential produced by the interaction of formation water, conductive drilling mud, and certain ion selective rocks such as shale. It is a recording versus depth of the difference between the electrical potential of a moveable electrode in the borehole and the electrical potential of a fixed surface electrode. Opposite shales, the SP curve usually defines a more or less straight line on the log, called the shale baseline. Opposite permeable formations, the curve shows deflections from the shale baseline. In thick beds, these deflections tend to reach an essentially constant deflection defining a sand line. The deflection may be due to the left (negative) or to the right (positive), depending primarily on the salinities of the formation water and of the mud filtrate. If the formation water is more saline than the mud filtrate and the deflection is to the left. If it is less saline than the mud filtrate, the deflection is to the right [9].

### Radioactivity logs [Gamma Ray Log (GR)]

Gamma ray log is a measurement of the natural radioactivity of the formation, the log normally reflects the shale content of the formation because the radioactive elements tend to concentrate in clays and shales. Clean formations usually have a very low level of radioactivity, unless a radioactive contaminant such as volcanic ash or granite wash is present or formation waters contain dissolved radioactive salts [9].

### Porosity Logs

Porosity is the ratio of void space in a rock to the total volume of rock, and reflects the fluid storage capacity of the reservoir [6]. Rock porosity can be obtained from the sonic log, the density log, or the neutron log. For all these logs, the tool response is affected by the formation porosity, fluid, and matrix. If the fluid and matrix effects are known or can be determined, the tool response can be related

to porosity. Therefore, these tools are often referred to as porosity logs [10].

### Density Log

The formation density log is a porosity log that measures the electron density of the formation [11]. The density log can assist to identify evaporite minerals, detect gas bearing zones, determine hydrocarbon density, and evaluate shaly-sand reservoirs and complex lithologies [8]. Formula used to determine porosity from density logs is given in the following [12].

$$\Phi_D = \frac{(\rho_{ma} - \rho_b)}{\rho_{ma} - \rho_f}$$

Where:  $\Phi_D$  = porosity by Density log,  $\rho_{ma}$  = matrix density,  $\rho_f$  = fluid density,  $\rho_b$  = bulk density.

### Neutron Log

According to [10] Neutron logs are used principally for delineation of porous formations and determination of their porosity. They respond primarily to the amount of hydrogen in the formation. Thus, in clean formations whose pores are filled with water or oil, the neutron log reflects the amount of liquid-filled porosity.

### Sonic Log

Sonic log is a porosity log that measures interval transit time ( $\Delta t$ , delta t, or DT) of a compressional sound wave traveling through the formation along the axis of the borehole. The interval transit time ( $\Delta t$ ) is dependent upon both lithology and porosity. time-average equation has been used in this study [13].

$$\theta S = \frac{\Delta t_{log} - \Delta t_{ma}}{\Delta t_{fl} - \Delta t_{ma}}$$

Where:  $\theta S$  = sonic-derived porosity,  $\Delta t_{fl}$  = interval transit time in the pore fluid (saltwater mud= 185  $\mu\text{sec}/\text{ft}$ ),  $\Delta t_{ma}$  = interval transit time of rock matrix,  $\Delta t_{log}$  = interval transit time measured by the Log

### Determination of Porosity

#### Total porosity

Total porosity is defined as the ratio of the volume of all the pores to the bulk volume of a material, regardless of whether or not all of the pores are interconnected [14].

[15] proposed an equation to compute the total porosity from neutron and density logs that may be expressed as.

$$\phi_t = \frac{\phi_N + \phi_D}{2}$$

#### Effective porosity

Effective porosity is the ratio of the volume of interconnected pores to the total volume of reservoir rock [14]. It is also defined as the total porosity minus the clay-bound water and water held as porosity within the clays [16].

$$\phi_{eff} = \phi_t * (1 - V_{sh})$$

#### Primary and secondary Porosity

The primary porosity is the amount of pore presents in the sediment at time of deposition, or formed during sedimentation. It is usually a function of the amount of space between rock – forming grains [6]. The development of vugs and fractures as found in carbonate reservoir rocks is termed Secondary Porosity and it is a function of the depositional history and diagenesis of the rocks [14].

Figure-3 shows relation between the effective porosity (PHIE) and secondary porosity (PHI<sub>sec</sub>) in well HF-316. The secondary porosity in general is less than the effective porosity and can be neglected in the most intervals of formation. When secondary porosity is high it indicates the presence of diagenesis processes in the formation such as dolomatization and dissolution.

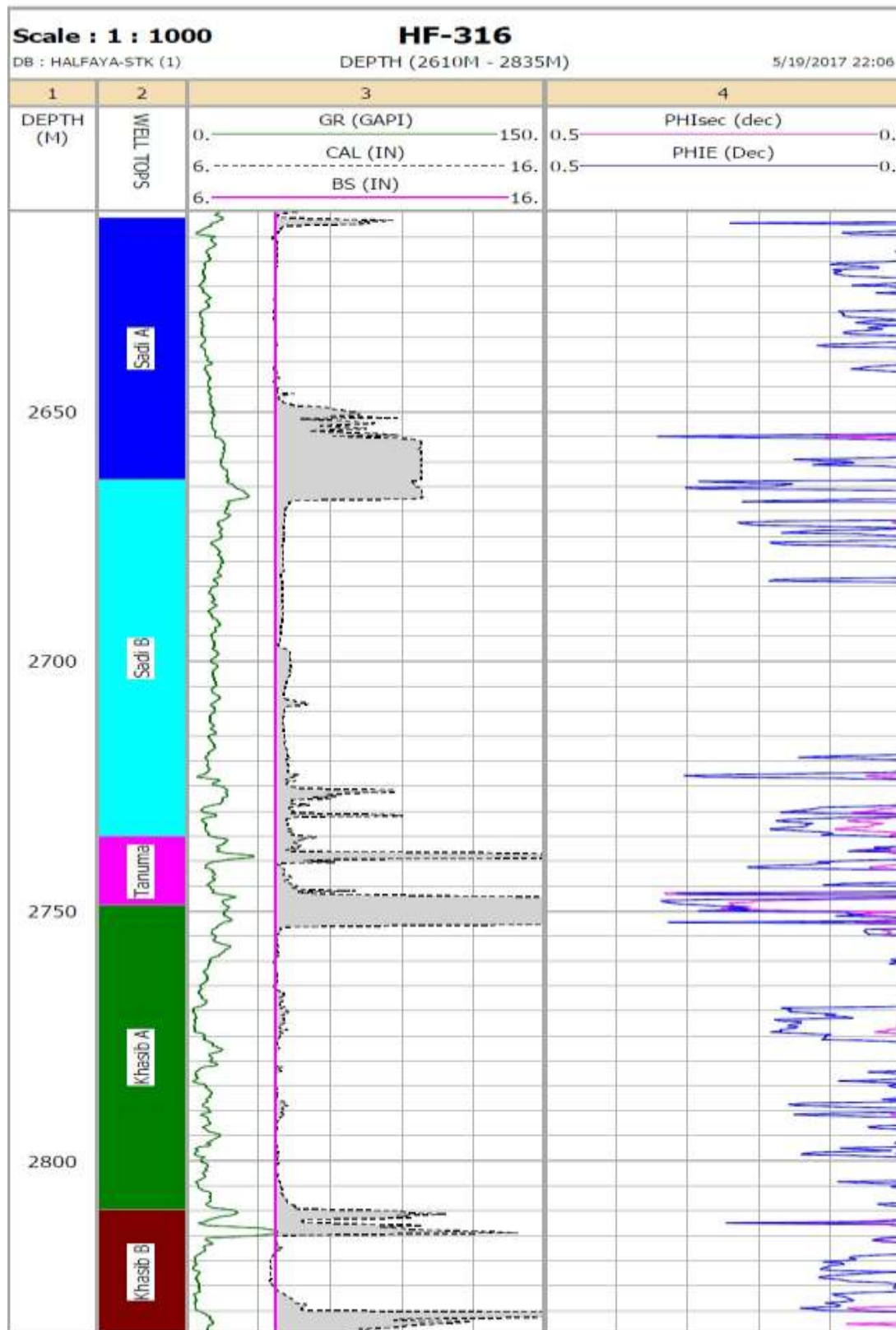


Figure 3-Effective and secondary porosity in wells HF-316.

### Determination of Lithology and Mineralogy

#### The Matrix Identification (MID) Plot

Indications of lithology, gas, and secondary porosity can also be obtained using the matrix identification (MID) plot. To use the MID plot, three data are required. First, apparent total porosity,

$\phi_{ta}$ , must be determined using the appropriate neutron-density and empirical (red curves) neutron-sonic crossplots [10].

The Figure-4 of MID cross plot show type of matrix in Khasib, Tanuma, and Sa'di formations at Halfaya Oil field that is mainly calcite.

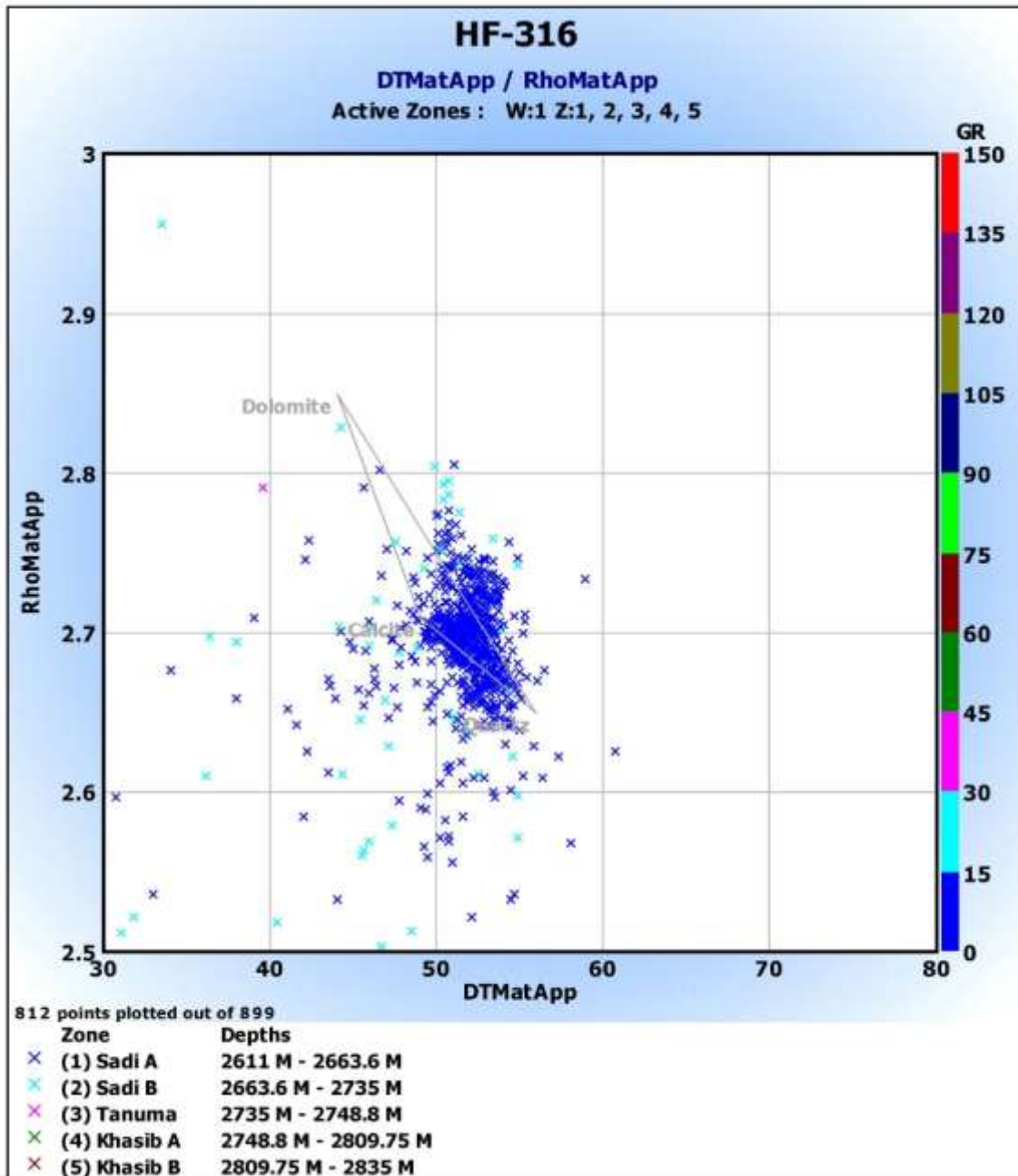


Figure 4-The MID cross plot for three formations in the well HF-316.

**M-N Cross Plot**

In more complex mineral mixtures, lithology interpretation is facilitated by use of the M-N plot. These plots combine the data of all three porosity logs to provide the lithology-dependent quantities M and N. M and N are simply the slopes of the individual lithology lines on the sonic-density and density-neutron crossplot charts, respectively. Thus, M and N are essentially independent of porosity, and a crossplot provides lithology identification [10].

The two calculated quantities are shown in two equations below.

$$M = \frac{\Delta t_f - \Delta t}{\rho_b - \rho_f} * 0.01$$

$$N = \frac{\Phi N_f - \Phi N}{\rho_b - \rho_f}$$

Where:  $\Delta t$  : interval transit time in th the formation,  $\Delta t_f$  : interval transit time in the fluid the formation,  $\rho_b$  : formation bulk density,  $\rho_f$  : fluid density,  $\Phi N$  : neutron porosity,  $\Phi N_f$  : neutron porosity of the fluid of the formation (usually=1.0).

The M-N cross plot for the reservoir units of Khasib, Tanuma, and Sa'di formation are illustrated in Figures-5. It has been observed that the Khasib, Tanuma, and Sa'di formation consists from limestone (represented by calcite region) with some dolomite. which is proved previously by (MID) cross plot and there is a clear direction for secondary porosity.

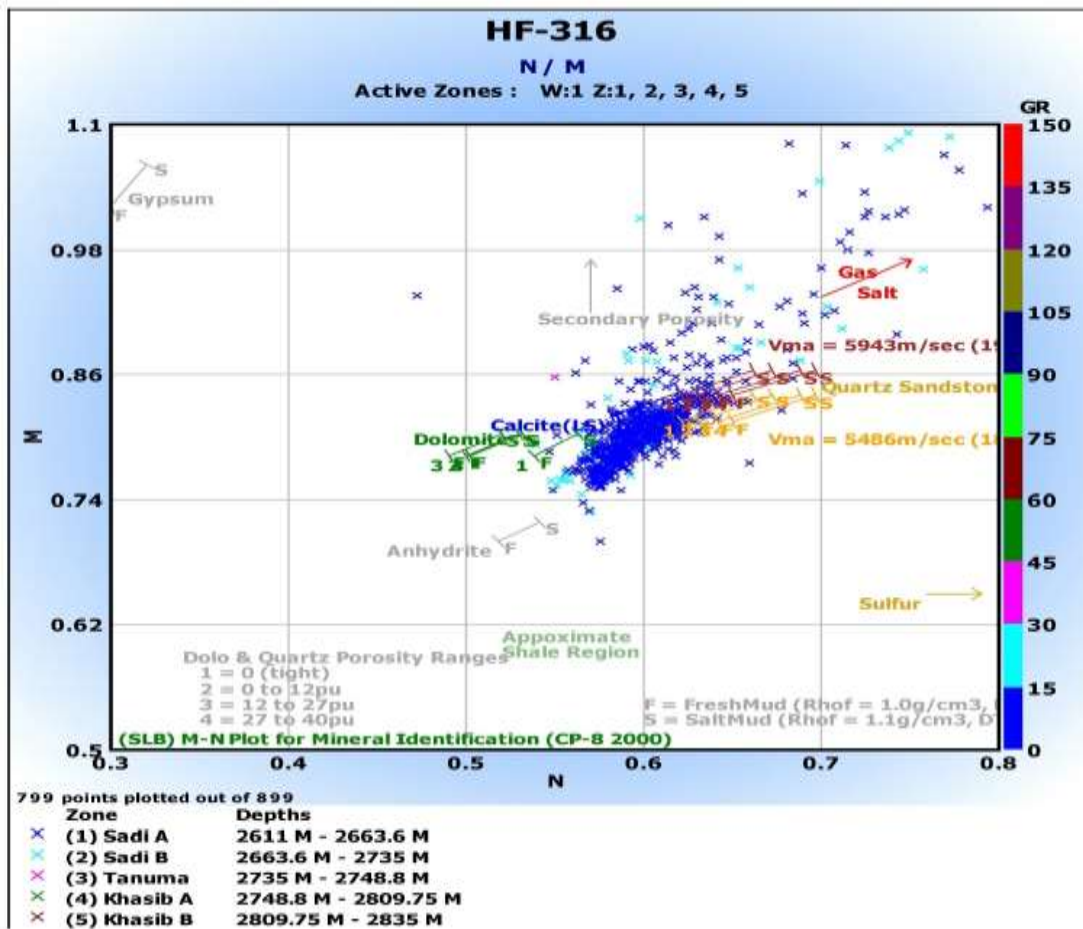


Figure 5-The M-N cross plot for well HF-158.

**Neutron density cross plotting**

The neutron–density cross plot is one of the oldest quantitative interpretation tools it was the principal method for determining the formation lithology [17]. The gamma ray log measures the natural radiation of a formation and primarily functions as a lithology log. It helps differentiate shales (high radioactivity) from sands, carbonates, and anhydrites (low radioactivity). The neutron log is a porosity device that is used to measure the amount of hydrogen in a formation, which is assumed to be related to porosity. The density log is a porosity device that measures electron density, and from that, formation bulk density. When these three logs are used together, lithologies can be determined [13]. Figures-(6, 7) illustrate in detail the lithology and averaged porosity of the two reservoir units (Khasib-A , Khasib-B) in well HF-316 in 2D. These figures show that nearly all the points of the reservoir units fall in the field of limestone which indicate the lithology of Khasib Formation with a little points of dolomite and with some shale.

Figures-(8, 9) illustrate in detail the lithology and averaged porosity of the two reservoir units (Tanuma and Sa'di) in 3D plot in well HF-316.

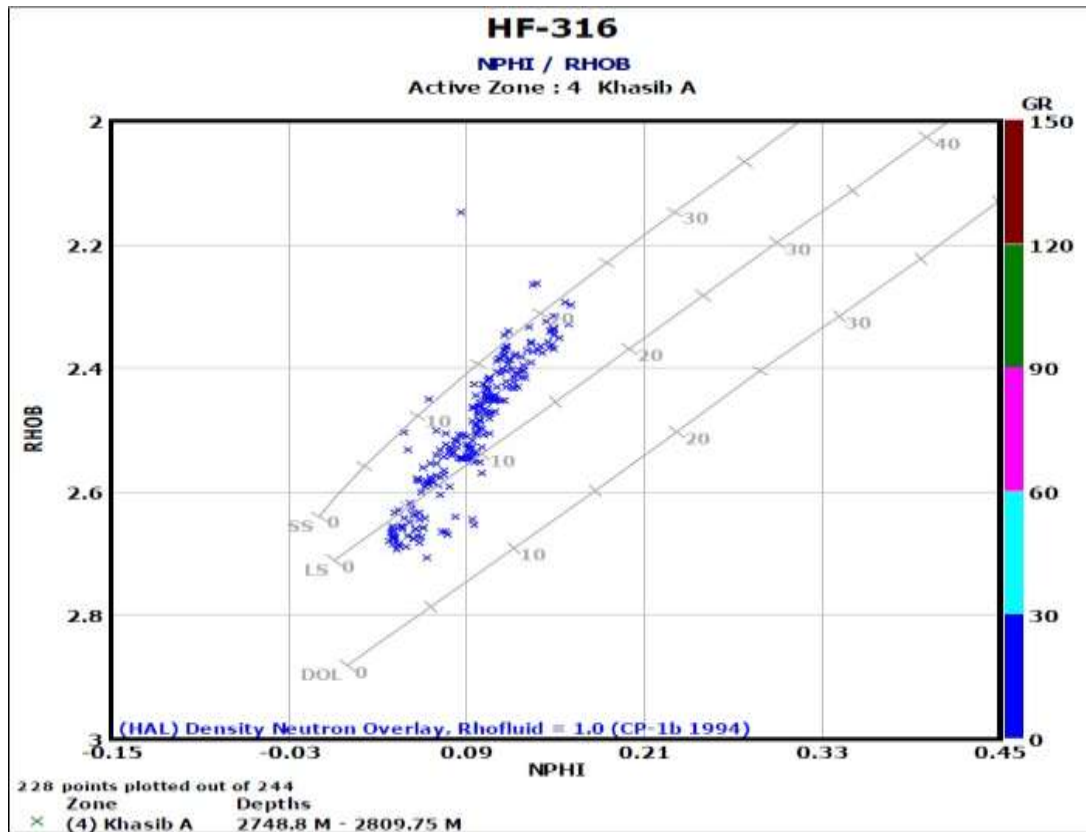


Figure 6-Shows the cross plot of  $\phi_N$  and  $\phi_D$  for well HF-316 in Khasib A.

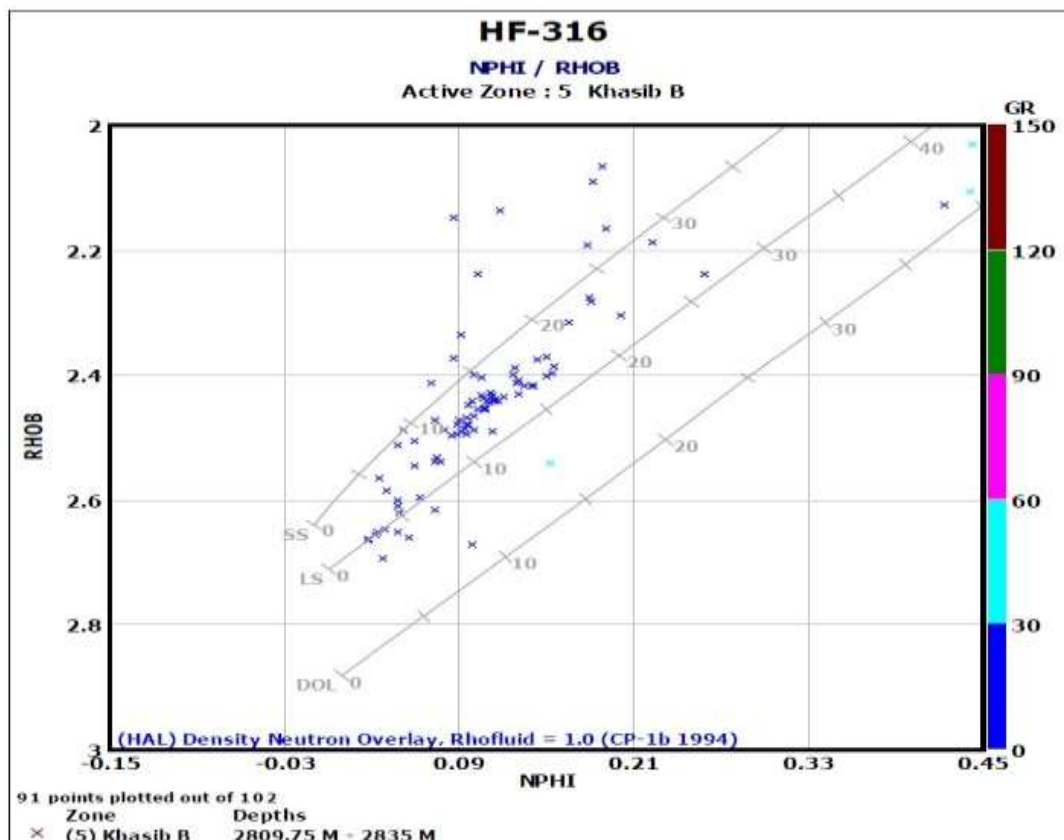


Figure 7-Shows the crossplot of  $\phi_N$  and  $\phi_D$  for well HF-316 in Khasib B

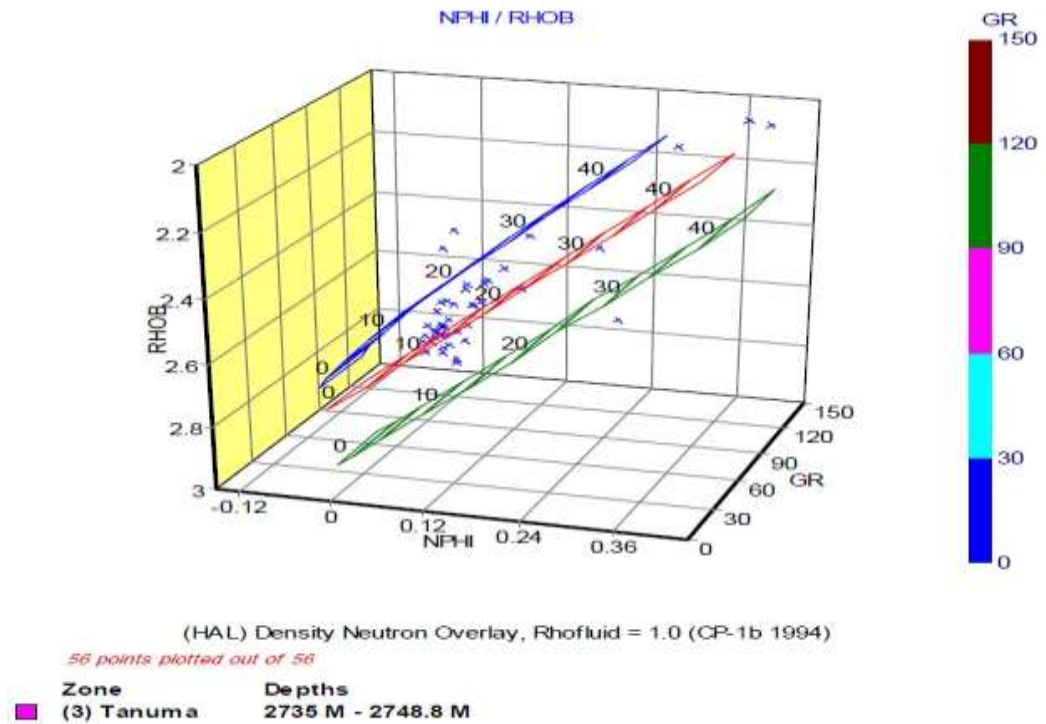


Figure 8-Shows the crossplot of  $\phi_N$  and  $\phi_D$  for well HF-316 in Tanuma Formation.

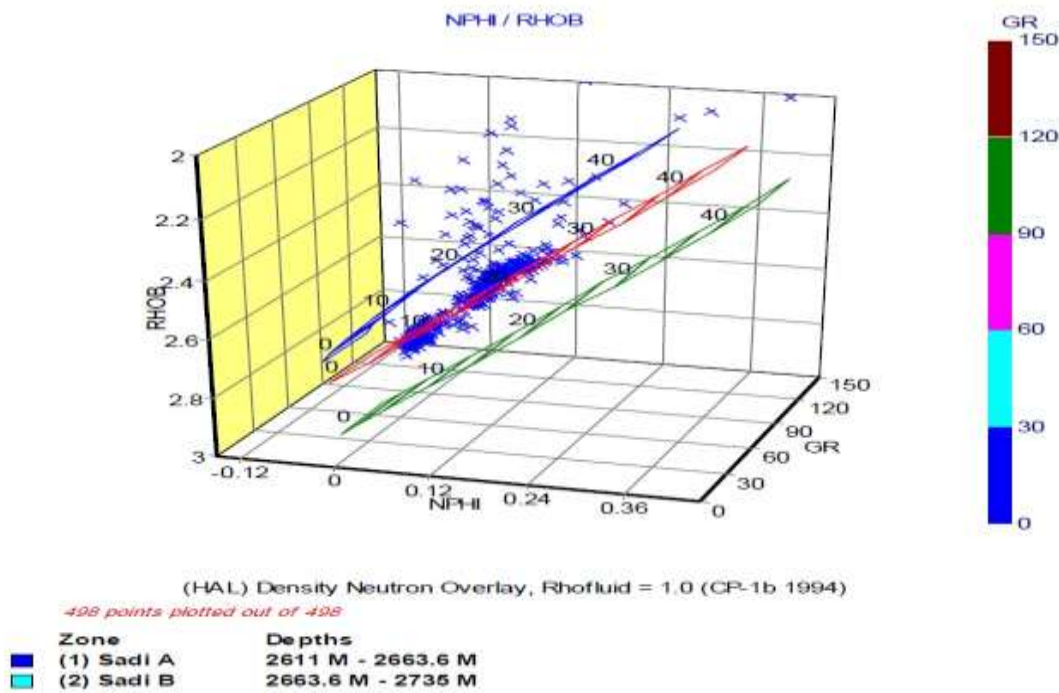


Figure 9-Shows the crossplot of  $\phi_N$  and  $\phi_D$  for well HF-316 in Sa'di Formation.

**Archie's Parameters (m, n, & a) Determination from well logs Using Pickett Plot**

The Pickett crossplot [18] is one of the simplest and most effective crossplot methods in use. This technique not only gives estimates of water saturation, but can also help to determine: (1) formation water resistivity ( $R_w$ ), (2) cementation factor (m), and (3) matrix parameters for porosity logs ( $\Delta t_{ma}$  and  $\rho_{ma}$ ) [19].

Pickett's plot has been used in determination of Archie's parameters from well log using Interactive Petrophysics software (V.3.5). [20] suggested a method that depends on a cross plot between resistivity vs. porosity to calculate (m) and/or (a) from well logs. The following logic describes this method. According to [20]:

$$R_t = \frac{a * R_w}{\phi^m * S_w^n}$$

Where:  $S_w$ : is the water saturation (fraction),  $R_w$ : is the water resistivity,  $\phi$ : is the porosity,  $R_t$  : Formation resistivity,  $a$ ,  $n$ , and  $m$ : Archie's parameters (dimensionless).

The three Archie's parameters (m, n, and a) were determined using Pickett plot. The Figures- (10,11, 12) show the results of Pickett's plot in HF-316.

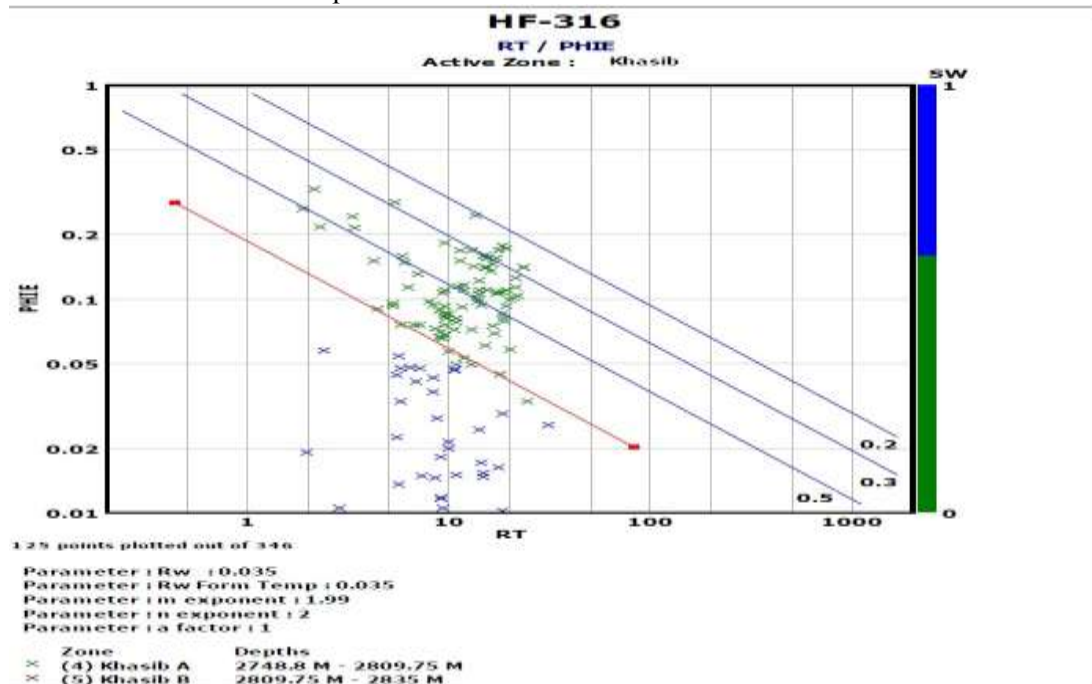


Figure 10-Pickett plot for Khasib Formation in well HF-316.

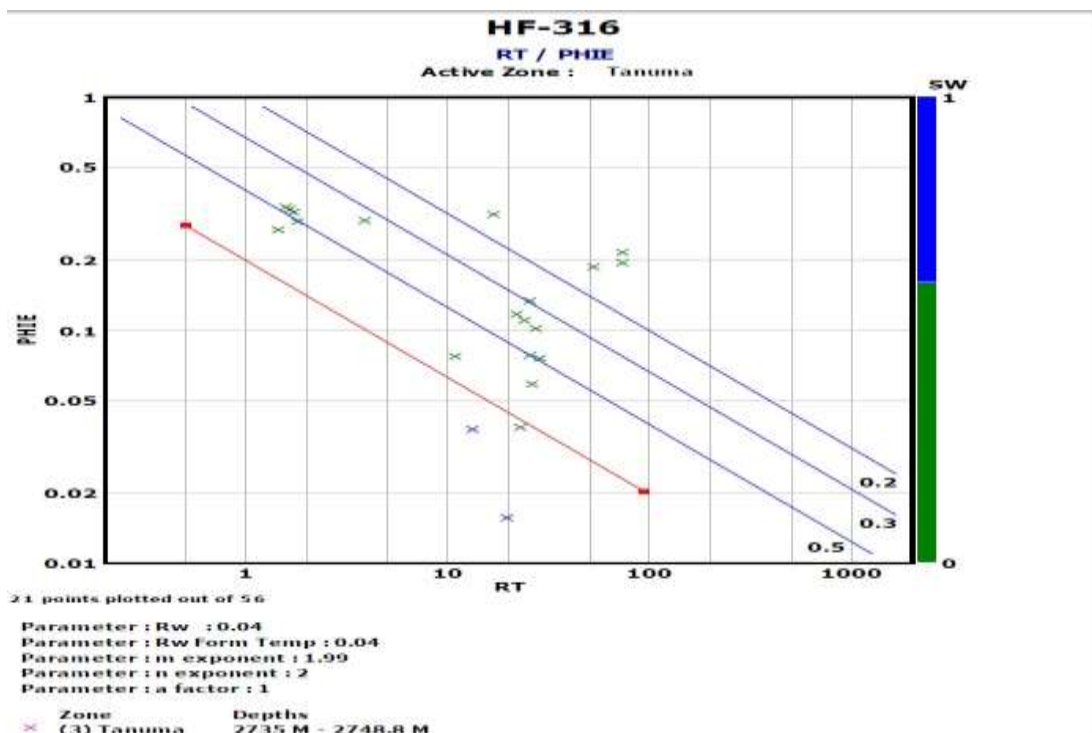


Figure 11-Pickett plot for Tanuma Formation in well HF-316.

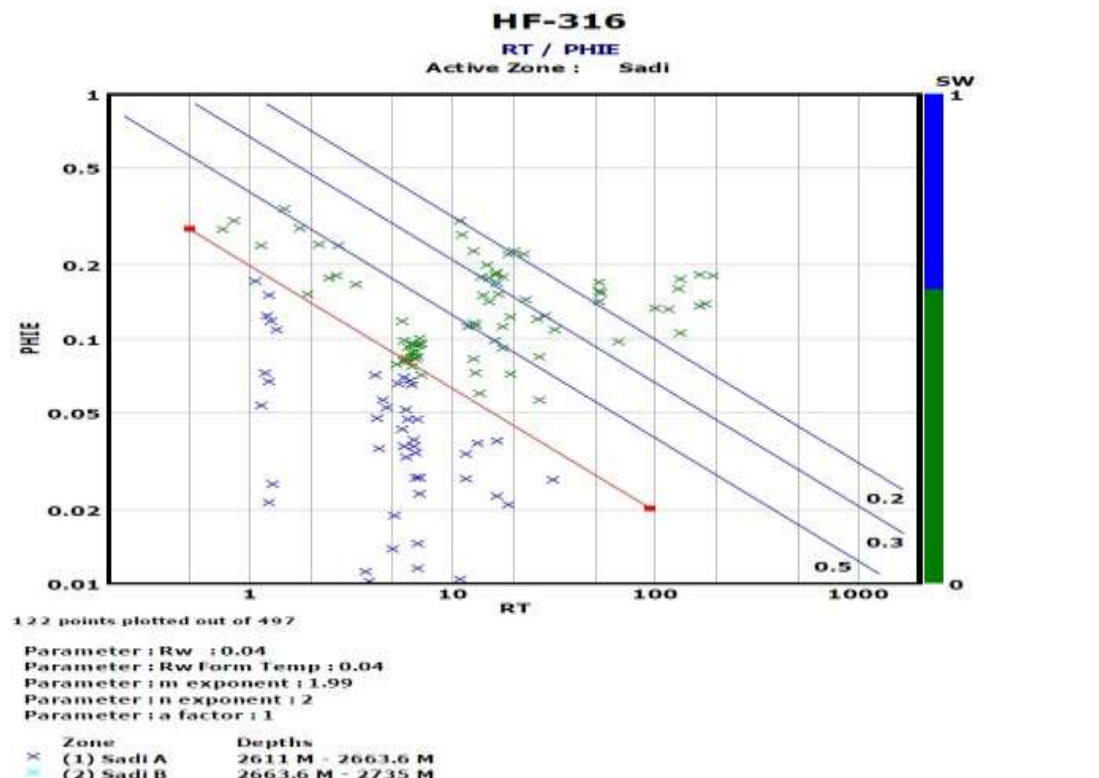


Figure 12-Pickett plot for Sa'di Formation in well HF-316.

**Water Saturation Determination (Archie's Method)**

According to [10] Archie determined experimentally that the water saturation of a clean formation can be expressed in terms of its true resistivity as:

$$S_w^n = \frac{FR_w}{R_t}$$

Where:  $R_w$ : water resistivity,  $R_t$  : true resistivity,  $F$  : formation resistivity factor  $n$  : saturation exponent

$F$  is usually obtained from the measured porosity of the formation through relationship [19]:

$$F = \frac{a}{\phi^m}$$

Where:  $m$ : is the cementation factor,  $a$ : is a constant.

In equation  $FR_w$ , is equal to  $R_o$ , the resistivity of the formation when 100% saturated with water of resistivity  $R_w$  [10].

$$S_w = \sqrt{\frac{R_o}{R_t}}$$

The water (mud filtrate) saturation,  $S_{xo}$  of the flushed zone can also be expressed by the Archie's formula [10]:

$$S_{xo} = \sqrt{\frac{FR_{mf}}{R_{xo}}}$$

Where:  $R_{mf}$ : resistivity of the mud filtrate and  $R_x$ ,  $R_{xo}$  : is the resistivity of the flushed zone.

**Movable and Residual Hydrocarbons**

According to [10] The saturation in the flushed zone can be used to estimate the residual oil saturation and the movable hydrocarbon saturation; depending on coefficients ( $m$ ,  $n$  and  $a$ ) from the  $R_t$ - $\phi$  crossplot.

The residual hydrocarbon saturation is equal to [21]:

$$S_{hr} = 1 - S_{xo}$$

Where:  $S_{hr}$ :The residual hydrocarbon saturation,  $S_{xo}$ : water saturation in the flushed zone.

The equation gives the saturation of unmoved or residual hydrocarbons in the invaded zone [21]. Comparison of  $S_{xo}$  and  $S_w$  in a hydrocarbon zone is considered to give movable hydrocarbons. It is equal to the fraction of movable hydrocarbons in the formation as shown in the equation below [21].

$$S_{hm} = S_{xo} - S_w$$

Where:  $S_{hm}$ : movable hydrocarbon saturation, fraction.

The percentage volume in terms of the reservoir is given by multiplying term by the porosity  $\phi$  [21].

The residual oil saturation and movable hydrocarbon are calculated from the following equations [22]:

$$S_{hr} = [\phi * (1 - S_{xo})]$$

$$S_{hm} = [\phi * (S_{xo} - S_w)]$$

Where is the Figure-13 which represents Computer Processed Interpretation (C.P.I) for HF-316

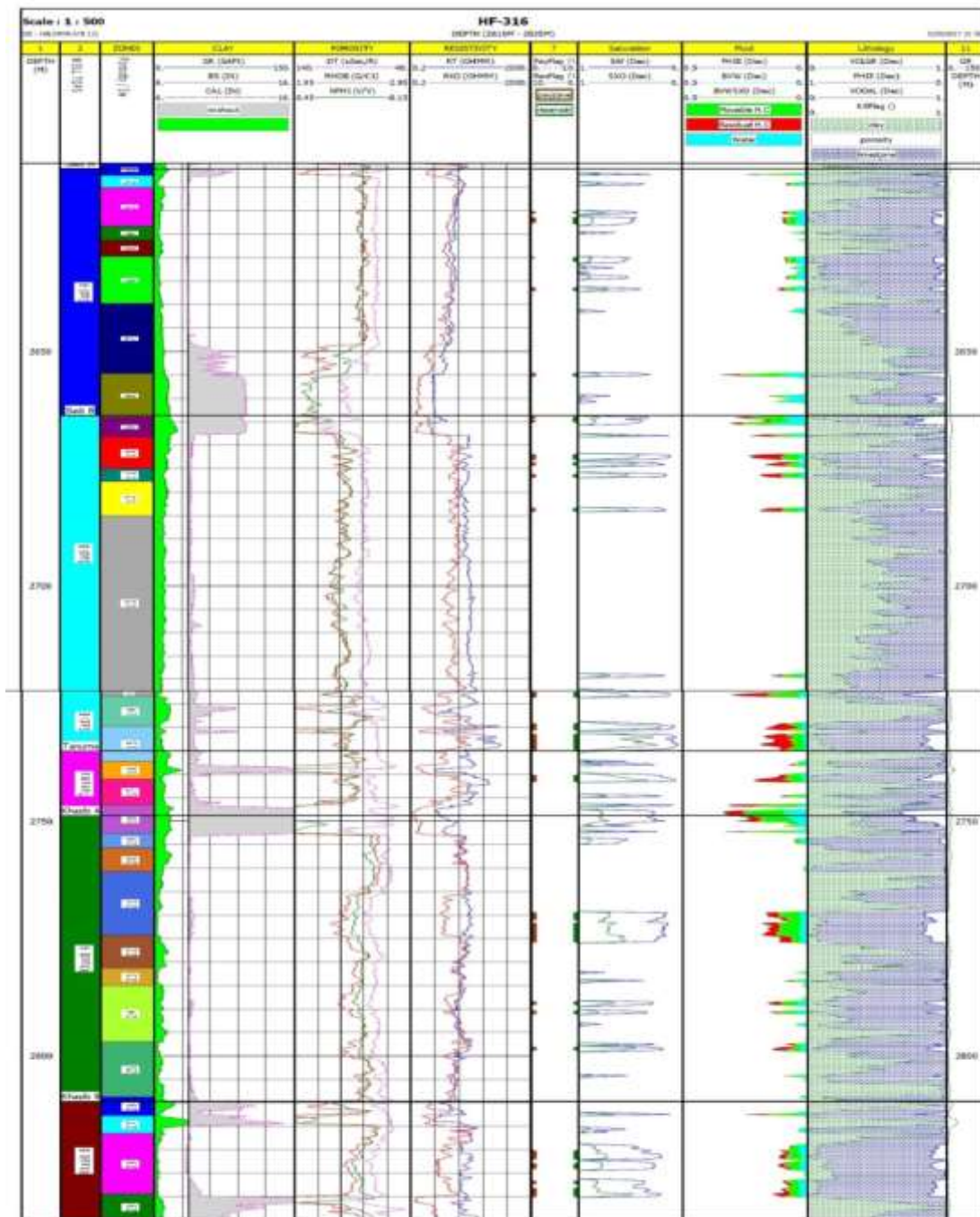


Figure 13-Computer Processed Interpretation (CPI) of well HF-316.

## Conclusions

1. Halfaya structure within Khasib, Tanuma, and Sa'di formations is composed of two domes extending from the north-west to the south-east.
2. Total porosity, effect porosity and secondary porosity have been calculated from neutron, density, and sonic logs. The secondary porosity in general is less than the effective porosity and can be neglected in the most intervals of formation. When secondary porosity is high it indicates the presence of diagenesis processes in the formation.
3. Lithology and mineralogy from The Matrix Identification (MID), and M-N Cross Plot indicated that the Khasib, Tanuma, and Sa'di formation consists from limestone (represented by calcite region) with some dolomite.
4. Archie's parameters were determined by using pickett's plot and found the range values of a, m and n are found to be (1), (1.85 – 1.99) and (2) respectively.
5. Computer Processed Interpretation (CPI) for wells of Halfaya oil field have been made using IP software. The computer processed interpretation showed that the Khasib Formation consists mainly of 2 reservoir units, Tanuma Formation consists of only one unit, and Sa'di Formation consists of 2 reservoir units separated by non-reservoir (barrier) beds.
6. Tanuma Formation represents the best reservoir in the study area. The Khasib Formation has better reservoir characteristic than Sa'adi Formation as identical by CPI log pattern.

## Recommendations

To increase the accuracy of the formation evaluation, new wells should be drilled using advanced and modern logging tools such as Electromagnetic Propagation Tool (EPT) log, Nuclear Magnetic Resonance (NMR) log, NMR log, etc. to get more confidential results. That drilling should be along the field and penetrate Khasib, Tanuma, and Sa'di formations to cover this area of the field.

## References

1. Aqrabi, A. A. M., Goff, J.C., Horbury, A.D. and Sadooni, F.N. **2010**. *The Petroleum Geology of Iraq*: Scientific Press.
2. Sharland, P. R., Archer, R., Casey, D. M., Davies, R. B., Hall, S. H., Heward, A. P., Horrury, A. D. and Simmons M. D. **2001**. *Arabian Plate Sequence Stratigraphy*, GeoArabia Special Publication 2, Gulf PetroLink, Bahrain, 371 p.
3. Buday, T. **1980**. *The regional geology of Iraq*. Stratigraphy and Paleogeography, Kassab, I.I. and Jassim, S.Z., (eds), Dar Al-Kutib Publ. House, Mosul, Iraq, P. 445.
4. Al-Ameri T. K., Al-Ekabi A. H, Al-Jawad S. N. **2014**. Palynomorph stratigraphy, palynofacies and organic geochemistry assessments for hydrocarbon generation of Ratawi Formation, Iraq. *Arab J Geosci*, 7(4): 1433–1455.
5. Schlumberger, **1989**. *Log Interpretation Principles/Applications*. Houston.
6. Halliburton, Energy Service, **2001**. *Basic Petroleum Geology and Log Analysis*: Houston, Texas, Halliburton Company. 80p.
7. Williams, M. E. M, Davis, R. K., Paillet, F. L., Turpening, R. M., Soul, S. J. Y., Schneider, G. W., **2009**. *Review of Borehole Based Geophysical Site Evaluation Tool and Techniques*. NWMO, Nuclear Waste Management Organization. Toronto, Ontario, Canada, 174p.
8. Schlumberger. **1972**. *Log Interpretation manual/principles*, Vol. I, Houston, Schlumberger well services Inc., 112 p.
9. Peters, E. J. **2006**. *Petrophysics*, Department of Petroleum and geosystems engineering, Texas, 1049p.
10. Schlumberger. **1998**. *Cased Hole Log Interpretation Principles/Applications*. Houston, Schlumberger Wireline and Testing.
11. Hughes, **1999**. *Petroleum Geology*. Houston, Texas, Baker Hughes INTEQ, 245p.
12. Desbrandes, R. **1985**. *Encyclopedia of Well Logging*. Gulf Publishing Company, 608 p.
13. Asquith, G. B. and Krygowski, D. **2004**. *Basic Well Log Analysis*. 2nd Edition: AAPG Methods in Exploration Series 16. Published by The American Association of Petroleum Geologists Tulsa, Oklahoma, 244p.
14. Bowen, D. G. **2003**. *Formation Evaluation and Petrophysics*. Core Laboratories, Jakarta, Indonesia 273p.
15. Schlumberger, **1974**. *Log Interpretation*, vol.II - Applications: New York.

16. Darlling T. **2005**. *Well Logging and Formation Evaluation*. Gulf Professional Publishing, Elsevier, USA, 326p.
17. Darwin V.E. and Singer, J.M. **2008**. *Well Logging for Earth Scientists*. 2nd Edition. Springer + Business Media B.V.
18. Pickett, G. R. **1972**. *Practical formation evaluation*: Golden Colorado, G. R. Pickett, Inc.
19. Asquith, G. and Gibson, CH. **1982**. *Basic Well Log Analysis for Geologists*. Methods in Exploration Series published by; The American Association of petroleum Geologists, Tulsa, Oklahoma USA.
20. Pickett, G.R. **1966**. Review of Current Techniques for Determination of Water Saturation from Logs. *Journal of Petroleum Technology*, (JPT), pp: 1425-1433.
21. Rider M. **2000**. *The geological interpretation of well logs*. Second edition, 280 p.
22. Serra O. **1986**. *Fundamentals of Well Log Interpretation Volume the Acquisition of Logging Data*. Developments in Petroleum Science, Elsevier, Amsterdam.